Cerebral Cortex November 2008;18:2666–2673
doi:10.1093/cercor/bhn023
Advance Access publication March 6, 2008

The Influence of Moderate Hypercapnia on Neural Activity in the Anesthetized Nonhuman Primate

A.C. Zappe[1], K. Uludağ[1], A. Oeltermann[1], K. Uğurbil[1,2] and N.K. Logothetis[1,3]

[1]Max-Planck Institute for Biological Cybernetics, Spemannstrasse 38, 72076 Tübingen, Germany, [2]Center for Magnetic Resonance Research University of Minnesota, Minneapolis, MN 55416, USA and [3]Imaging Science and Biomedical Engineering, University of Manchester, Manchester, UK

Hypercapnia is often used as vasodilatory challenge in clinical applications and basic research. In functional magnetic resonance imaging (fMRI), elevated CO_2 is applied to derive stimulus-induced changes in the cerebral rate of oxygen consumption ($CMRO_2$) by measuring cerebral blood flow and blood-oxygenation-level–dependent (BOLD) signal. Such methods, however, assume that hypercapnia has no direct effect on $CMRO_2$. In this study, we used combined intracortical recordings and fMRI in the visual cortex of anesthetized macaque monkeys to show that spontaneous neuronal activity is in fact significantly reduced by moderate hypercapnia. As expected, measurement of cerebral blood volume using an exogenous contrast agent and of BOLD signal showed that both are increased during hypercapnia. In contrast to this, spontaneous fluctuations of local field potentials in the beta and gamma frequency range as well as multiunit activity are reduced by ~15% during inhalation of 6% CO_2 ($pCO_2 = 56$ mmHg). A strong tendency toward a reduction of neuronal activity was also found at CO_2 inhalation of 3% ($pCO_2 = 45$ mmHg). This suggests that $CMRO_2$ might be reduced during hypercapnia and caution must be exercised when hypercapnia is applied to calibrate the BOLD signal.

Keywords: cerebral cortex, extracellular recording, fMRI, macaque, metabolism, neurovascular coupling, striate cortex

Introduction

Most functional imaging techniques rely on the fact that regional cerebral blood flow (CBF), cerebral blood volume (CBV), and the cerebral metabolic rate of oxygen consumption ($CMRO_2$) are directly related to brain function (Roy and Sherrington 1890). The mechanisms of the dynamic neurovascular coupling can be investigated by studying the relationship of hemodynamic responses to a sensory stimulus. Vascular challenges such as hypoxia and hypercapnia are interesting alternatives to such sensory stimulation, because they elicit hemodynamic responses that are not derived from modulations of neuronal activity alone. An elevation of partial pressure of CO_2 (pCO_2) increases CBF mainly by an unspecific decrease of pH. Hypercapnia might therefore be used to distinguish between the effects of changes in CBF and CBV on hemodynamics and those due to stimulus-induced neural activation and subsequent increases in $CMRO_2$.

Hypercapnic challenge has been used in a number of attempts to calculate stimulus-induced changes in oxygen metabolism from combined CBF and blood-oxygenation-level–dependent (BOLD) data using functional magnetic resonance imaging (fMRI) (Davis et al. 1998; Kim et al. 1999; Schwarzbauer and Heinke 1999). Like many neuroimaging methods that rely on hemodynamics, the BOLD contrast mechanism also depends on more than one physiological parameter, namely CBF, CBV, and $CMRO_2$; the interactions among these parameters remain poorly understood (e.g., Buxton et al. 2004). Experiments assessing the individual contributions of CBF, CBV, and $CMRO_2$ to the BOLD signal have, therefore, been of particular interest because they promise to shed light on its physiological basis.

The effect of hypercapnia on both hemodynamics and metabolism was already in the focus of research decades ago. Beginning in the early 1940s, Kety and Schmidt (Kety and Schmidt 1945) developed the nitrous oxide technique, which made it possible to measure global and later local $CMRO_2$ changes in vivo. Early studies with this technique reported that $CMRO_2$ remains constant under moderate hypercapnic challenge (Kety and Schmidt 1947; Novack et al. 1953; Krnjevic et al. 1965; Nilsson and Siesjoe 1976) although high intersubject variability was observed. Other studies using a number of different techniques showed either a decrease (Metzger and Heuber 1977; Kliefoth et al. 1979; Balestrino and Somjen 1988; Sicard and Duong 2005) or even an increase in $CMRO_2$ during hypercapnia (Horvath et al. 1994; Jones et al. 2005). Such contradictory observations are most likely due to differences in experimental design, including the species and sensitivity of the method.

Recently, numerous investigations have used the $CMRO_2$ formula derived by Davis et al. (Davis et al. 1998; Hoge et al. 1999; Kim et al. 1999; Kastrup et al. 2002; Uludag et al. 2004) to investigate the associations between hemodynamic and metabolic changes in response to various stimuli. Yet, this approach assumes that the elevated pCO_2 has no direct effects on $CMRO_2$ itself. The validity of this assumption has yet to be established. It has been suggested (Siesjoe 1980) that the experimental results available on this effect are ambiguous. It has been shown, for example, that moderate and severe hypercapnia does indeed increase the threshold for electrically and chemically induced seizures (Aram and Lodge 1987; Balestrino and Somjen 1988). In fact, this effect is exploited by physicians to suppress epileptic seizures. In addition, very high CO_2 tension (>20% CO_2 inhalation) may have a sedative action or even induce anesthesia (Capps 1968).

$CMRO_2$ is directly related to regional neural activity (Siesjoe 1978). The effects of hypercapnia on neuronal activity would therefore indicate changes in $CMRO_2$. The present study combines, for the first time, intracortical recordings of spontaneous neural activity with concurrent measurements of hemodynamics with MRI in the visual cortex of anesthetized macaque monkeys during hypercapnia. We show that spontaneous activity is reduced by mild and moderate hypercapnia, suggesting that the basic assumption of the CMRO2 formula

(Davis et al. 1998) is not valid under our experimental conditions. In contrast, the BOLD signal and CBV are increased during hypercapnia. Taken together, the data reveal that hypercapnia-induced increases in CBF are accompanied by decreases in neuronal activity. In other words, CO_2 exerts opposing effects on neuronal activity and CBF, yielding a pattern of signal changes that is entirely different from that observed during sensory stimulation (Logothetis et al. 2001). Possible methodological corrections in the calibration of the BOLD signal are presented which take into account the observed changes in neural activity. A preliminary version of these results has been presented in abstract form (Zappe et al. 2005).

Material and Methods

Experimental Setup

Experiments were conducted in a vertical 4.7-Tesla scanner with a 40-cm-diameter bore (BioSpec 4.7 T/40 cm, Bruker Medical, Ettlingen, Germany). The system has a 50 mT/m (rise time < 180 μs) actively shielded gradient coil (Bruker, BGA 26) of 26 cm inner diameter. Three healthy adult monkeys (*Macaca mulatta*, 4–6 kg) were investigated in 10 separate sessions. All sessions were approved by the local authorities (Regierungspräsidium) and were in full compliance with the guidelines of the European Community for the care and use of laboratory animals (EUVD 86/609/EEC). The experiments were performed under general anesthesia in accordance with previously published protocols (Logothetis et al. 1999). The conditions of our anesthesia were tested for stress in the animal and for strength, variability, and reproducibility of the BOLD signal in various areas (Logothetis et al. 1999; Kayser et al. 2005). Briefly, the animal was intubated after intravenous administration of fentanyl (31 μg/kg), thiopental (5 mg/kg), and succinyl choline chloride (3 mg/kg). Each eye was treated with 2 drops of 1% cyclopentolate hydrochloride to achieve mydriasis, and then fitted with hard contact lenses (Firma Wohlk, Kiel, Germany). Mivacurium chloride (3–6 mg/kg/h) was used after induction to assure complete paralysis of the eye muscles during anesthesia. Anesthesia was maintained with remifentanil (0.5–2 μg/kg/min) and vital monitors continuously monitored the following vital functions: ECG, blood pressure, end-tidal pCO_2, SpO_2, and temperature. Respiration was maintained at a ventilation rate of ~1.4 L/min, 24 strokes/min and oxygen saturation over 95%. The baseline value for end-tidal pCO_2 was adjusted to 33 mmHg, which had been determined previously to be optimal for BOLD studies compared with the value in the awake monkey ~40–42 mmHg (Logothetis et al. 1999). Throughout the experiment, lactate Ringer's with 2.5% glucose was infused at 10 ml/kg/h and body temperature was maintained at 38–39 °C.

Hypercapnic conditions were induced by switching ventilation from air to premixed medical gases composed of 21% O_2 combined with either 3% or 6% CO_2 and balanced N_2 (Westfalen AG, Münster, Germany, analytical accuracy ± 2% relative). End-tidal pCO_2 was increased by approximately 12 ± 2 mmHg and 23 ± 4 mmHg for 3% and 6% CO_2, respectively. The level of end-tidal pCO_2 was compared with arterial pCO_2 by sampling from the femoral artery (ABL500, Radiometer, Copenhagen, Denmark); both were consistent within 1 standard deviation (n = 3). Arterial oxygen saturation was evaluated in the blood gases as well as tissue oxygen saturation with oximetry and both showed no significant changes during hypercapnia. Within each session, normocapnia and 2 levels of hypercapnic states were interleaved; for example, 0%/3%/0%/6%/0%. Usually 2–4 repetitions of each hypercapnic state per day could be accomplished. We designated the first 7 min after the onset of CO_2 inhalation the *transient hypercapnic phase,* as the end-tidal pCO_2 values during this phase continued to increase. Hypercapnia was kept stable for approximately 10 minutes before switching back to medical air.

fMRI was performed with a 25 mm surface coil, acquiring 2-shot gradient-echo echo planar imaging pulse sequences with time repetition/time echo = 250/16 ms and flip angle = 20°. Two axial slices were collected at 0.75 × 0.75 mm^2 in-plane resolution and 2-mm thickness. In addition, an anatomical scan was acquired to visualize the location of the electrode tip in the cortex (FLASH sequence TR/TE 2000/8.5 ms, 0.5-mm slice thickness, 187.5 × 187.5 μm^2, see Fig. 1). In 2 of the sessions, CBV imaging with monocrystalline iron oxide nanocolloid (MION) was performed in order to assess blood volume changes in the small parenchymal vessels (Mandeville et al. 1998; Mandeville and Marota 1999). MION was injected intravenously at the end of the session (8 mg/kg, citrate-buffered), which suppressed the MR signal in striate cortex (area V1) to ~50% of preinjection levels. After waiting 5-min postinjection for signal stabilization, CBV imaging was performed using the same MR parameters as in BOLD imaging. BOLD data on the *transient hypercapnic phase* were obtained in 18 scans recorded in 5 sessions and 3 animals. The CBV time course of the *transient hypercapnic phase* was obtained in 2 scans on 2 different sessions and animals.

Electrical recordings were performed within the operculum of V1, where a 2-mm trepanation was performed at the beginning of each experimental session. We designed and custom-built the electrodes with an impedance of 500–800 kΩ using platinum–iridium ($Pt_{90}Ir_{10,}$ Ø 125 μm) wire, which was beveled and glass-coated (Corning glass 7570). At the beginning of each session the electrode was lowered into layers III–V of striate cortex such that a stable response to visual stimulation was obtained. The position of the electrode was verified in an anatomical scan of the MR. In sessions recording with 2 electrodes, the second electrode was inserted at an angle of 8° to the first electrode with 3–5 mm between the tips (in average 3.9 mm, see Fig. 1).

Electrophysiological recordings were carried out by measuring current rather than voltage changes (Logothetis et al. 2001). Specifically, current flow from the electrode tip was measured over a total cable length of 6 m and converted into voltage at the input stage of the amplifier, with all circuitry located outside the magnetic field. Signals were amplified by 10–30 mV/pA. The method of reducing gradient interference on electrophysiological recording and thus allowing signal recovery by postprocessing has been described elsewhere (Logothetis et al. 2001; Oeltermann et al. 2007). Briefly, induction voltages in the electrode caused by switching on the MR gradient coil were compensated on-line. Two types of interference compensation were necessary: First, the induced currents in the animal were measured with a rotational symmetric sensor placed around the electrode and the sign-inverted current passed back to the animal via a mouth electrode. In the case of 2 electrodes the compensatory current measured at each electrode cannot be passed to a single mouth electrode. Instead, the mouth electrode was connected to global

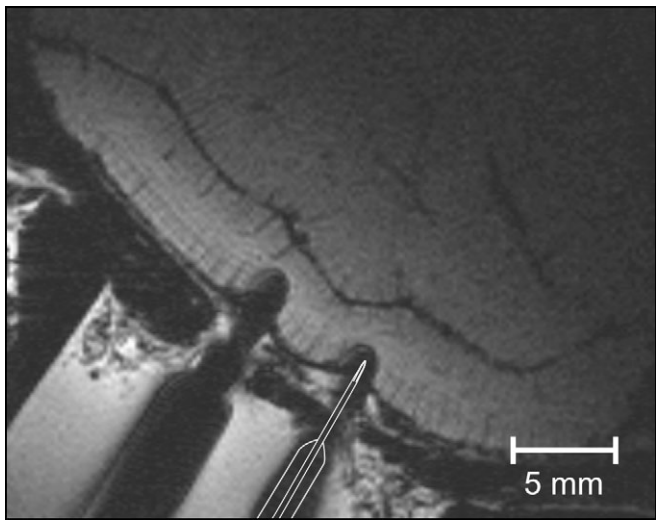

Figure 1. Anatomical slice showing 2 electrodes positioned in gray matter of macaque V1. The image was obtained after infusion of MION and as a consequence vessels and especially the intracortical veins appear dark. The distance between the electrodes is ~5 mm. The outline of the electrode appears artificially enlarged because of the susceptibility artifact. Thus, the real dimensions of the electrode are indicated by a sketch at the right penetration site.

ground and the sign-inverted current was passed back to each electrode holder. Second, the voltages induced in the electrode holder and near the electrode had to be compensated. With the help of a pickup sensor at the gradient wires these interferences could be estimated and subtracted from the electrode signal. For 2-electrode recordings, both electrodes were compensated by individual sensors.

The functional modulation of hemodynamics and evoked neuronal activity were monitored under normocapnia between every hypercapnic challenge with a visual stimulus to decide whether to include those data into the final analysis. One out of 10 sessions did not show significant stimulus modulation in either of the modalities and was thus excluded from further analysis. Altogether 57 repetitions of normocapnia were performed, and inhalation of 3% and 6% was repeated 25 and 26 times, respectively (5 sessions with one electrode, 4 sessions with 2 electrodes). The *transient hypercapnic phase* was recorded during 5 sessions and 20 repetitions (all these sessions included 2 electrodes).

Visual stimuli were presented using a super video graphics array fiber-optic system (AVOTEC, Silent Vision) with 640 × 480 resolution and a 60 Hz frame rate. The stimulus pattern consisted of a rotating polar checkerboard pattern (~2.5 Hz visual modulation at 100% contrast). The direction of rotation reversed every 1.5 s to reduce neural adaptation. A stimulus block consisted of 12.5 s presenting a black screen was followed by 12.5-s visual stimulation and again 39-s presentation of a black screen.

Data Analysis

Five frequency bands were extracted with finite impulse response filters and rectified to obtain the envelope of the signal. Theta in the range of 4–8 Hz, low-pass at 2 Hz; alpha in the range of 8–14 Hz, low-pass at 3 Hz; beta in the range of 14–24 Hz, low-pass at 4 Hz; gamma in the range of 24–90 Hz, low-pass at 30 Hz; multiunit activity (MUA) in the range of 400–3000 Hz, low-pass at 30 Hz. The neuronal signal is split up into these 5 frequency bands, which are based on the electroencephalography literature. A more meaningful selection of frequency bands is currently under investigation in our lab and could differ substantially from these frequency bands. Their description is not yet complete, so we will limit ourselves to giving our results in terms of these "classical" bands. As shown in the supplementary information to Logothetis et al. (2001), the transfer function of the system is not constant but depresses lower frequencies in comparison to MUA. This can be compensated for by integrating the signal, yielding a flat transfer function. We tested the effect of the transfer function by comparing the results with integrated and nonintegrated signals for 2 sessions. The integrated signals were only slightly different and counterbalanced in the 2 sessions tested; we assume that the transfer function did not bias the results. In the analysis presented here the nonintegrated signals were used.

The root-mean-square of each band was computed and a correction was performed to account for linear trends, hysteresis, and rebound effects. This step was necessary as baseline activity over long time periods (several hours) was analyzed, and the signals could be neither normalized nor centered. Equal numbers of scans under each condition (normocapnia/hypercapnia) were grouped within each session and normalized to the mean signal level of normocapnia on that particular day. In 2-electrode sessions, the data from 2 channels were averaged before averaging across different experimental sessions. The results for each electrode separately are given under Supplementary Material. When averaging the normalized signals across sessions, the sessions were not weighted with their number of repetitions, because intersession variability was higher than intrasession variability. Errors were calculated as the standard deviation of the normalized mean across sessions. If not stated otherwise, the default significance level was taken to be $P < 0.005$ (2-tailed, paired, Student's *t*-test). The electrophysiological response during the *transient hypercapnic phase* was also low-pass filtered at 1 Hz to improve visualization.

FMRI data were analyzed using self-written MATLAB codes (The MathWorks Inc., Natick, MA). After normalization, the data were first detrended and then wavelet filtered to remove temporal noise. As the animals were artificially ventilated with a constant respiration rate, respiratory artifacts could easily be removed by filtering. The scans recorded directly after the onset of CO_2 inhalation to capture the *transient hypercapnia phase* were normalized without any filtering. Subsequently, regions of interest restricted to primary visual cortex excluding the voxels with electrode susceptibility artifacts were manually identified on the basis of the anatomical image. Their time courses were extracted and converted to percent change. The amplitude of the functional BOLD signal (only acquired under normocapnia as a control) was calculated from the power of the stimulus frequency including the first harmonics. It was monitored over the day to ensure that the functional hemodynamic response remained intact.

The Formula for Calibrated BOLD

For the same CBF change for visual and hypercapnic stimulation, a larger BOLD signal change is obtained for the hypercapnic than for the visual response. This indicates a lower oxygen saturation of hemoglobin and hence a greater $CMRO_2$ change during stimulation. Davis et al. introduced a formula with which changes in $CMRO_2$ during stimulation can be calculated on the basis of measured CBF and BOLD signal changes evoked by hypercapnia and visual stimulation (Davis et al. 1998). This so-called *calibrated BOLD* approach assumes no $CMRO_2$ changes under hypercapnia (Davis et al. 1998; Hoge et al. 1999; Kastrup et al. 2002; Liu et al. 2004; Stefanovic et al. 2006; Chiarelli, Bulte, Piechnik, et al. 2007a; Leontiev and Buxton 2007). The estimate of $CMRO_2$ is based on the equation derived by Davis et al., which relates the CBF and $CMRO_2$ to the BOLD signal change ΔS (Davis et al., 1998):

$$\Delta S(\%) = A\left(1 - f^{\alpha-\beta} m^{\beta}\right)$$

In the steady state, α is the exponent that relates the CBV to CBF with a power law expression and was previously determined from steady-state studies in the rhesus monkey to be 0.38 (Grubb et al., 1974). The term f and m are CBF and $CMRO_2$ normalized to their respective baseline values. The CBF–CBV relationship was established in rhesus monkeys under hypercapnia and hyperventilation and Ito et al. (2001, 2003) as well as Jones et al. (2002) have observed this relationship to be similar both under hypercapnia and sensory stimulation in humans and rats. Note that in this equation CBV represents the blood volume containing deoxygenated hemoglobin, that is, mainly venous CBV at lower magnetic fields, whereas α relates the total CBV to CBF. However, as shown by many studies, the results on $CMRO_2$ are relatively insensitive to the exact value of α (Chiarelli, Bulte, Piechnik, et al. 2007a). Because of this and because the fractional change of venous CBV is not known, we adopt for the following calculation the value of α for total CBV.

The term β is a numerical parameter that expresses the superlinear dependence of the relaxation rate on the deoxyhemoglobin concentration in blood and is calculated from simulations to be 1.5 for a magnetic field strength of 1.5 T (Davis et al., 1998). The local parameter A is a calibration constant and corresponds to the maximum BOLD change for complete absence of deoxyhemoglobin.

To calculate the consequences of altered $CMRO_2$ by hypercapnia, we first assume different values for $\Delta CMRO_2$ during hypercapnia and calculate the corresponding calibration constant A (see equation above) from exemplary published BOLD/CBF data during hypercapnia. Second, with this derived A and the corresponding stimulus-evoked BOLD and CBF changes, we calculate the stimulus-induced $\Delta CMRO_2$. Third, we calculate the ratio of ΔCBF and $\Delta CMRO_2$ during stimulation, the so-called coupling constant n (Uludag et al. 2004).

Results

Three bands of electrophysiological recordings were found to be significantly depressed under hypercapnia compared with normocapnia. The gamma band decreased to 97.5 ± 4% and 84.7 ± 4% for 3% and 6% CO_2 mixtures, respectively; MUA to 96.3 ± 7% and 85.3 ± 5%, and beta to 97.4 ± 5% and 89.8 ± 8% respectively (Fig. 2*A*). Although not significant (one tailed *t*-test), a trend toward reduced spontaneous activity was observed for 3% CO_2 (for gamma: $P < 0.11$, for MUA: $P < 0.11$ and for beta: $P < 0.14$). The change in spontaneous activity for 6% CO_2 was significant at $P < 0.0005$ in all 3 frequency

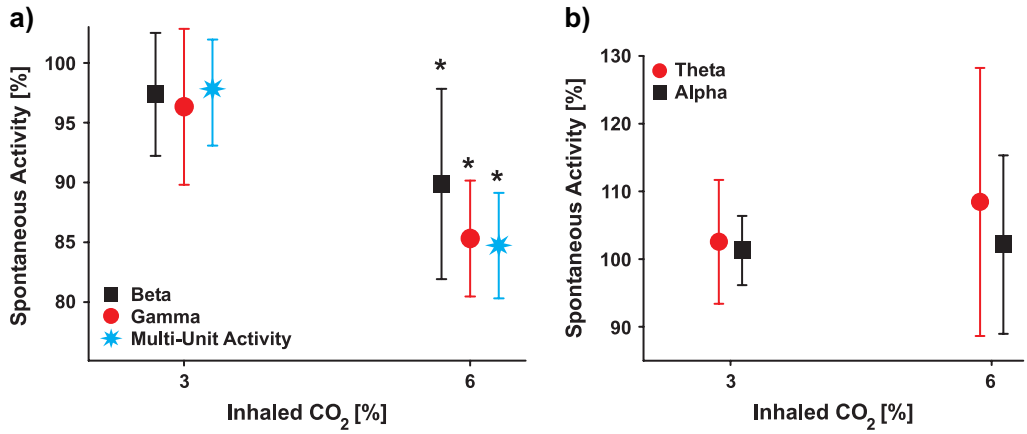

Figure 2. Spontaneous activity without stimulus presentation during 3% and 6% CO_2 administration. (*A*) Gamma band decreased to 97.5 ± 4% and 84.7 ± 4%, beta band to 97.5 ± 5% and 89.9 ± 8% and MUA to 96.3 ± 6% and 85.3 ± 5% for the 2 levels of CO_2 inhalation (n = 9). The change in spontaneous activity in these 3 bands is highly significant for 6% CO_2 ($P < 0.0005$). For 3% CO_2, a trend toward neuronal activity reduction is visible ($P \sim 0.1$). (*B*) Theta and alpha bands do not change under mild and moderate hypercapnia (*P* between 0.2 and 0.6). *Depicts significant changes.

bands. In addition, the decreases at this level were consistently reproducible in all sessions. During the mildest hypercapnic level tested (3% CO_2), the MUAs were significantly reduced in only 4 out of 9 sessions (~10% average reduction) (Table 1). Similar results were observed for beta and gamma range activity of local field potentials. The theta and alpha bands remained unaffected for both mild and moderate hypercapnia with a *P* value between 0.2 and 0.6 (Fig. 2*B*).

The first 6 min of gamma and MUA activity directly after the onset of 6% CO_2 inhalation are depicted in Figure 3 (*transient hypercapnia phase*). For display purposes, the time course of beta activity is not shown. The beta band showed the same trend as the gamma and MUA bands, but the time course has lower signal-to-noise ratio (compare Fig. 2*A*). In particular, the time courses vary greatly from session to session and over electrodes within a session. In 2 out of 5 sessions the decrease was found to be stronger for MUA than for the gamma range. In the remaining sessions the changes were of comparable size. For the onset of 3% CO_2 none of the 3 bands showed significant decreases.

As expected, for both 3% and 6% hypercapnia challenges, the BOLD signal and the CBV increased (i.e., the T_2^*-weighted MR signal in the presence of MION decreased). During 6% CO_2 administration, the BOLD signal was found to increase by 2.5 ± 0.3% (n = 5) and CBV-related MR signals were found to decrease by 23 ± 1% (n = 2) (see Fig. 4). This increase in CBV corresponds to a concomitant CBF increase which in this range can be approximated by a linear relationship with the slope of 0.38 resulting in ~60% CBF change (Grubb et al. 1974; Lee et al. 2001), in agreement with our previous study which resulted in 60–100% CBF change for 6% CO_2 (Zappe et al. 2008).

In the following, we illustrate how the estimation of $CMRO_2$ calculated by *calibrated BOLD* is affected for 2 data sets; one study with a rather small CBF change around 18% by Davis et al. (1998) and a second data set with a larger CBF change of up to 80% by Stefanovic et al. (2006). In the study by Davis et al. (1998), the BOLD signal and CBF changed during hypercapnia by 1.8% and 18%, respectively, and during visual stimulation by 1.7% and 45%; in the study by Stefanovic et al. (Fig. 5 in 2006) changes of ΔBOLD = 3.7% and ΔCBF = 80% can be found during hypercapnia and ΔBOLD = 2.7% and ΔCBF = 90% during visual stimulation. Using the algorithm described in Methods, the resulting coupling constant n is shown in Figure 5 as a function of $\Delta CMRO_2$ during hypercapnia. As can be seen, a $CMRO_2$ decrease during hypercapnia leads to an increase in the calculated coupling constant n, that is, leads to a smaller calculated $\Delta CMRO_2$ for the same ΔCBF during stimulation. In other words, the larger the reduction in $CMRO_2$ during hypercapnia is, the larger is the estimate of n during stimulation.

To estimate a correct coupling constant n, it is crucial to know the amount by which $CMRO_2$ is affected by the applied hypercapnic challenge. Previous results suggest that CBF increases by approx. 90% during inhalation of 6% CO_2 (ΔpCO_2 = 22 mmHg) (Reivich 1964; Grubb et al. 1974) or 50% increase in CBF for 5% CO2 inhalation (ΔpCO_2 = 11 mmHg). To provide an estimate of the impact our findings can have on the ΔCBF to ΔCMRO2 ratio, we assume that the upper limit of $\Delta CMRO_2$ correspond to the reduction in gamma and MUA power. The data shown in Figure 3 show a decrease of 15% for both gamma power and MUA for 6% CO_2 inhalation which we, for sake of simplicity, translate into a ~15% $CMRO_2$ decrease for a 90% CBF increase. Although the effects of CO_2 on CBF and $CMRO_2$ are probably neurochemically independent, both reflect the amount of CO_2 applied. We therefore assume a linear relationship between the hypercapnia-induced effect on CBF and $CMRO_2$ and estimate a 1% reduction in $CMRO_2$ for every 6% increase in CBF. In the study of Davis et al., hypercapnia induced only an 18% CBF increase, which according to our findings implies a 3% decrease in total $CMRO_2$ (Davis et al. 1998); for the 80% CBF increase in the study by Stefanovic et al. (2006), our simulations suggest a 13.3% decrease in total $CMRO_2$. From the estimation shown in Figure 5, this leads to new coupling constants of ~3.2 and ~7.7 during stimulation compared with the previously estimated ~2.6 and ~4.3 for the study by Davis et al. and Stefanovic et al., respectively. These estimates give an *upper* limit for the impact of the hypercapnia-induced $CMRO_2$ decrease on the calculation of the coupling constant for 2 studies in the literature and the same estimation procedure can also be done for other calibrated BOLD studies.

Discussion

In this study, we report the first simultaneous measurements of neural and hemodynamic signals during mild and moderate

Table 1

Single-subject MUA data for normocapnia, mild and moderate hypercapnia. The error given is the coefficient of variation within session

Session	MUA under normocapnia, mild, and moderate hypercapnia									
	i04vp1	j04xm1	j04zv1	j04yz1	b05qr1	j04x41	b05xe1	i04wx1	i04ze1	
CO_2 = 0%	100 ± 5	100 ± 1	100 ± 11	100 ± 7	100 ± 1	100 ± 3	100 ± 1	100 ± 5	100 ± 2	(%)
CO_2 = 3%	86* ± 7	90* ± 3	91 ± 1	92*	100 ± 1	101 ± 12	101 ± 1	102 ± 10	103*	(%)
CO_2 = 6%	74* ± 8	83 ± 24	87 ± 3	88* ± 5	86* ± 1	88* ± 7	90 ± 15	86 ± 13	85*	(%)

Note: All numbers are normalized to normocapnia in each individual session.

*Indicates significantly different changes. Standard deviations are given as error, but in 3 cases only one repetition of this particular condition was available and thus no error was estimated.

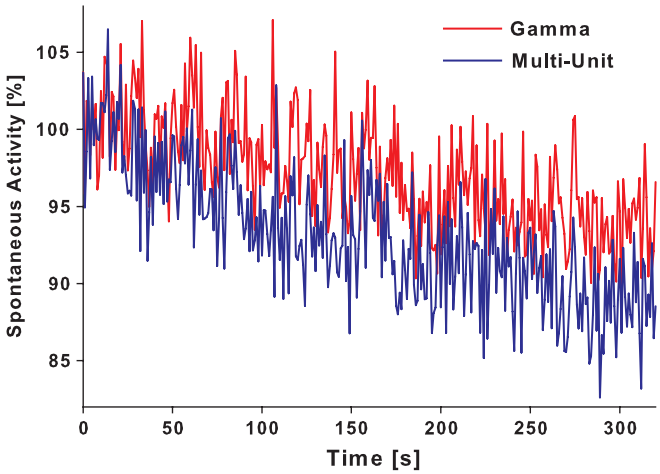

Figure 3. The averaged time course of gamma and MUA electrophysiological responses after the onset of 6% CO_2 inhalation. In 2 out of 5 sessions, the amplitude of change was much stronger for MUA than for gamma range, which was still visible in the group average. The beta band was noisier and thus not included in the figure.

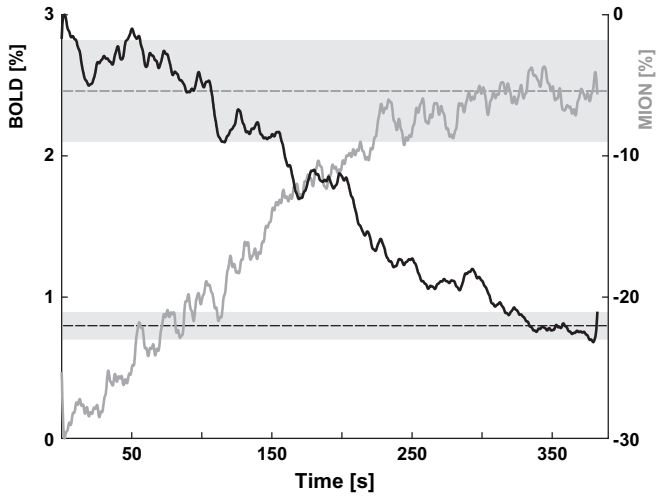

Figure 4. Time course of BOLD (gray) and MION (black) signals in primary visual cortex after the onset of 6% CO_2 inhalation. The dotted lines give the saturation levels with the standard deviation of the saturation level shown as shaded boxes.

hypercapnia (3% and 6% inspired CO_2) in the macaque monkey. In agreement with previous research (Bandettini and Wong 1997; Kastrup et al. 1999; Gaohong et al. 2002; Jones et al. 2005; Sicard and Duong 2005) we found that hemodynamic signals, as assessed with BOLD signal and CBV fMRI using MION, showed a clear increase during hypercapnia. We used visual stimulation during the normocapnic periods and found that increased pCO_2 had no long-lasting effects on functional signal modulation following the hypercapnic episode. Local field potentials, MUA and BOLD signals were increased in parallel by the visual stimulus in all normocapnic periods between periods of hypercapnia (data not shown), indicating that the stimulus-induced neuronal and vascular responses are intact. A hypercapnia-related decrease in deoxyhemoglobin content per unit volume of brain corresponding to the BOLD signal increase can be due either to enhanced CBF or to decreased $CMRO_2$. On the basis of the BOLD data alone, it is impossible to distinguish between the effects of a CBF increase and those of a $CMRO_2$ decrease, because the BOLD signal is sensitive to the ratio of these parameters.

In addition, the magnitudes of local field potentials in the gamma and beta frequency ranges and MUA were significantly reduced at the 6% CO_2 level with respect to their baseline values. For 3% inspired CO_2, these neuronal signals were significantly reduced in 4 out of 9 sessions, with the remaining 5 showing no significant change in any of the frequency bands. For 3% CO_2 only a trend toward a decreased signal was present. Overall, the decrease in neuronal baseline activity during moderate hypercapnia (i.e., 6% CO_2) was accompanied by an increase in hemodynamic signals; this is opposite to the pattern of changes observed during stimulation.

The effects of pCO_2 in blood on neuronal activity and oxidative metabolism have been the subject of intensive discussion. The data presented here support earlier reports proposing that neural activity is affected by changes in pCO_2, albeit without offering insights into the mechanism by which hypercapnia may be affecting neurons or glia. One potential mechanism is a pH change, as suggested by several investigators (Kliefoth et al. 1979; Balestrino and Somjen 1988; Brian 1998; Dulla et al. 2005). Because CO_2 diffuses throughout tissue space as a dissolved gas and readily combines with water to form carbonic acid, the pH is reduced in both intra- and extracellular space to a degree that depends on the local buffering capacity. In turn, this has an effect on neuronal excitability, thereby reducing spiking and synaptic activity. This was already experimentally demonstrated in brain slices (Folbergrova et al. 1972; Tombaugh and Sapolsky 1990). In addition, Balestrino and Somjen suggest that pH changes might not be the only effect of CO_2 impacting neuronal excitability. They hypothesize that CO_2 has an additional (and more direct) effect on the neuronal membrane. However, presuming intact neurovascular coupling, a reduction in neuronal activity should lead to a decrease in the CBF and BOLD signal. In contrast, cerebral arteries are relaxed by increased pCO_2, resulting in increased CBF by a direct and/or an indirect effect of CO_2 on vascular (endothelium and smooth muscle) and extravascular

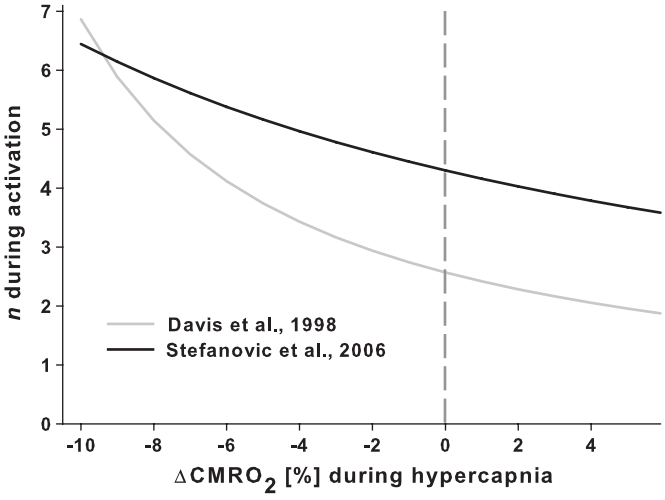

Figure 5. Model calculation shows how the coupling constant *n* between fractional changes of CBF and $CMRO_2$ would be affected if spontaneous activity and hence $CMRO_2$ is altered by hypercapnia, illustrated here with data taken from the literature (Davis et al. 1998; Stefanovic et al. 2006). The gray line at 0% $CMRO_2$ indicates the value assumed by the calibrated BOLD approach.

cells (perivascular nerves, parenchymal neurons, and glia) (Azin 1981; Wang et al. 1994; You et al. 1994).

Whatever the mechanism may be, our direct neurophysiological measurements suggest that neural activity is altered under moderate hypercapnia under conditions that are commonly used for BOLD calibration. Other approaches exist in addition to the previously described *calibrated BOLD* approach to calculate $CMRO_2$ with MR: e.g. inhalation of O^{17} (Zhu et al. 2002), calibration with 1H MRS (Kida et al. 2000; Hyder et al. 2001), and global parameterization of the BOLD normalization factor (Kim and Ugurbil 1997) based on a method developed by Ogawa et al. (1992). Very recently, Chiarelli and colleagues (Chiarelli, Bulte, Wise et al., 2007b) introduced hyperoxia challenge to calibrate BOLD. However, they did not perform any functional stimulation. Despite the alternatives using MRI, calibration of BOLD by means of hypercapnia challenge is hitherto the most commonly used and relatively easy-to-implement method and might in principle enable an estimation of neural activity from the hemodynamic responses. The coupling constant *n* reported by *calibrated BOLD* falls mainly between 1.6 (Liu et al. 2004) and 3.5 (Kastrup et al. 2002; Sicard and Duong 2005). Also positron emission tomography has been used to determine the coupling constant. Several studies found inconsistent values for *n* ranging from 1 to 10 (for overview see Gjedde et al. 2002).

For the estimation of the coupling constant *n*, we assumed that $CMRO_2$ decreases in parallel to gamma band and MUA. This concomitant $CMRO_2$ changes might be smaller than the measured gamma and MUA changes, however, it is very unlikely that there is no decrease in $CMRO_2$, given that both local field potentials and MUA are depressed. Note that, it remains for future investigations to find out what the quantitative relationship between oxidative metabolism and electrophysiological processes and signals is. Our findings of a reduction of neuronal activity and presumably $CMRO_2$ have consequences for the *calibrated BOLD* approach, namely, that the coupling constant *n* between fractional changes in CBF and $CMRO_2$ is larger than previously calculated.

In the study of Sicard and Duong (2005), the authors investigate baseline as well as stimulus-induced CBF, BOLD, and $CMRO_2$ in the anesthetized rat under hypercapnia. They calculate no changes in baseline $CMRO_2$ nor stimulus-induced $\Delta CMRO_2$ for 5% CO_2 inhalation, and a trend for a decrease in baseline $CMRO_2$ and almost no stimulus-induced $\Delta CMRO_2$ for 10% inspired CO_2. However, recalculating baseline $CMRO_2$ using CBF and BOLD changes induced by hyperoxia also presented in their study, yields a decrease in baseline $CMRO_2$ in both CO_2 challenges in agreement with our results.

The human studies discussed above and our present study in monkeys differ mainly in species and anesthetics. It is known that anesthesia can have a major impact on both the functional (Brewer et al. 2002) and the response (Sicard et al. 2003), as well as the temporal characteristics (Brevard et al. 2003) depending on the agent and concentration used. Therefore, it is important to note that the CBF responsiveness to hypercapnia under remifentanil anesthesia has been shown to be intact in humans (Klimscha et al. 2003; Pattinson et al. 2006) although a slowing down of the hemodynamic response curve to hypercapnia cannot be excluded (Brevard et al. 2003). Remifentanyl, however, could have a vasoconstrictive effect and thus decrease the basal CBF level in gray matter of the occipital lobe (Klimscha et al. 2003), which should not affect the findings of this study. The hypercapnia-induced increased CBV could potentially lead to a depressant effect of the intravenously infused anesthetic agent itself. This is very unlikely for the following reasons: 1) One of the authors of the current study (N.K.L.) has complete electrophysiological data sets with varying concentrations of remifentanil. The data were acquired by a collaborator interested in the effects of different types of anesthesia on neural responses (an SFN abstract, Fust et al. 2003, and on-going Ph.D. thesis). In contrast to barbiturate and isoflurane anesthesia, no changes in activity in striate and extra striate cortex are observed over a large range of remifentanil concentration. 2) The magnitude of sensory stimulus-induced CBF changes is similar to those induced by hypercapnia. If the pure CBF increase leads to depressed activity, this should also be observed under sensory stimulation. As far as we know, this has not been reported in the literature.

Besides any direct effects of the anesthesic agent, the anesthesia we use requires pressure-controlled ventilation of the monkey. Awake humans tend to increase their respiration rate when inhaling CO_2 and thus are able to decrease their end-tidal pCO_2 in comparison to a mechanically ventilated subject with the same inhaled CO_2 concentration. Therefore, the inspired CO_2 concentration might not always be a fair comparison between experiments, but the end-tidal pCO_2 could indeed be a better way to compare studies. Taking a rough estimate from literature, the end-tidal pCO_2 values for 3% CO_2 in our setup are comparable with 5–6% CO_2 inhalation in humans, whereas 6% CO_2 is more comparable with 10% CO_2. Furthermore, the mechanical ventilation allows us to select a level of baseline end-tidal pCO_2 other than the normal value in an awake subject. In this study, we adjust baseline end-tidal pCO_2 to 33 mmHg which is around 9 mmHg below the normal level in an awake monkey, because this gives optimal BOLD signal (Logothetis et al. 1999). We compared the effects between 3% and 6% CO_2 inhalation and found the decrease in the gamma band and MUA still to be significant at $P < 0.001$ and the beta band at $P = 0.03$. As the significant changes in neural activity take place between 3% and 6% CO_2, this does not alter our main findings. Note that the end-tidal pCO_2 changes in this

study (~23 mmHg for up to 10 min) were higher than those used in most prior human experiments, but comparable levels have been reported (e.g., Stefanovic et al. 2006; ΔpCO_2 ~23 mmHg for 1–3 min). Experiments with awake nonhuman primates are necessary to resolve whether the anesthetic agent and respiratory ventilation interfere with hypercapnia.

Conclusions

We have demonstrated that already moderate hypercapnia has an opposite effect on CBF and neural activity in the anesthetized nonhuman primate. This pattern is contrary to that observed during sensory stimulation (Logothetis et al. 2001) and can be explained by independent effects of CO_2 on neuronal activity and blood vessels. Drugs or substances like caffeine, nicotine and alcohol might also have a dissociative effect on neuronal activity and hemodynamics, as has been suggested by various investigators using indirect measurements of neuronal activity (Cameron et al. 1990; Levin et al. 1998; Jacobsen et al. 2002). Investigating such dissociations will be useful both for the study of the neural basis of hemodynamic responses and for the study of the activity of the agents themselves on the central nervous system. Finally, using model calculations, we have also shown here that caution needs to be exercised when applying hypercapnia to calibrate the BOLD signal because the assumption of no change in $CMRO_2$ during hypercapnia can lead to erroneous $CMRO_2$ estimates during stimulation. However, the *calibrated BOLD* approach can still be applied provided that hypercapnia-induced effects on $CMRO_2$ are monitored and, if necessary, taken into account.

Supplementary Material

Supplementary material can be found at: http://www.cercor.oxfordjournals.org/

Funding

Max-Planck Society.

Notes

We would like to thank our colleagues Mark Augath and Yusuke Murayama for technical support with these experiments. We are grateful to Bruno Weber at the University hospital in Zürich, Schwitzerland, for many inspiring discussions and for help with blood sampling from the femoral artery and Michael Schmid at the National Institute of Mental Health in Bethesda, USA, for giving insights on the application of MION. MION was obtained from the Center for Molecular Imaging Research, Massachusetts General Hospital, Boston, USA. *Conflict of Interest*: None declared.

Address correspondence to Anne-Catherin Zappe, Max-Planck Institute for Biological Cybernetics, Spemannstr 38, 72076 Tübingen, Germany. Email: aczappe@tuebingen.mpg.de.

References

Aram JA, Lodge D. 1987. Epileptiform activity induced by alkalosis in rat neocortical slices: block by antagonists of N-methyl-D-aspartate. Neurosci Lett. 83:345–350.

Azin AL. 1981. Role of pH in the mechanism of action of CO2 on smooth muscle of the cerebral arteries. Bull Exp Biol Med. 91:411.

Balestrino M, Somjen GG. 1988. Concentration of carbon dioxide, interstitial pH and synaptic transmission in hippocampal formation of the rat. J Physiol. 396:247–266.

Bandettini PA, Wong EC. 1997. A hypercapnia-based normalization method for improved spatial localization of human brain activation with fMRI. NMR Biomed. 10:197–203.

Brevard ME, Duong TQ, King JA, Ferris CF. 2003. Changes in MRI signal intensity during hypercapnic challenge under conscious and anesthetized conditions. Magn Reson Imaging. 21:995–1001.

Brewer AA, Press WA, Logothetis NK, Wandell BA. 2002. Visual areas in macaque cortex measured using functional magnetic resonance imaging. J Neurosci. 22:10416–10426.

Brian JE, Jr. 1998. Carbon dioxide and the cerebral circulation. Anesthesiology. 88:1365–1386.

Buxton RB, Uludag K, Dubowitz DJ, Liu TT. 2004. Modeling the hemodynamic response to brain activation. Neuroimage. 23(Suppl 1): S220–233.

Cameron OG, Modell JG, Hariharan M. 1990. Caffeine and human cerebral blood flow: a positron emission tomography study. Life Sci. 47:1141–1146.

Capps RT. 1968. Carbon dioxide. Clin Anesth. 3:122–134.

Chiarelli PA, Bulte DP, Piechnik S, Jezzard P. 2007a. Sources of systematic bias in hypercapnia-calibrated functional MRI estimation of oxygen metabolism. Neuroimage. 34:35–43.

Chiarelli PA, Bulte DP, Wise R, Gallichan D, Jezzard P. 2007b. A calibration method for quantitative BOLD fMRI based on hyperoxia. Neuroimage. 37:808–820.

Davis TL, Kwong KK, Weisskoff RM, Rosen BR. 1998. Calibrated functional MRI: mapping the dynamics of oxidative metabolism. Proc Natl Acad Sci USA. 95:1834–1839.

Dulla CG, Dobelis P, Pearson T, Frenguelli BG, Staley KJ, Masino SA. 2005. Adenosine and ATP Link PCO2 to cortical excitability via pH. Neuron. 48:1011.

Folbergrova J, MacMillan V, Siesjoe BK. 1972. The effect of hypercapnic acidosis upon some glycolytic and Krebs cycle-associated intermediates in the rat brain. J Neurochem. 19:2507–2517.

Fust A, Pauls J, Augath M, Murayama Y, Oeltermann A, Logothetis NK. The influence of anaesthetic agents on neural activity in visual cortex revealed by electrophysiology and high-resolution functional MRI. 33rd Society for Neuroscience Meeting. 69:14.

Gaohong W, Feng L, Zhu L, Xiaoli Z, Shi-Jiang L. 2002. Transient relationships among BOLD, CBV, and CBF changes in rat brain as detected by functional MRI. Magn Reson Med. 48:987–993.

Gjedde A, Marrett S, Vafaee M. 2002. Oxidative and nonoxidative metabolism of excited neurons and astrocytes. J Cereb Blood Flow Metab. 22:1–14.

Grubb RL, Jr, Raichle ME, Eichling JO, Ter-Pogossian MM. 1974. The effects of changes in PaCO2 on cerebral blood volume, blood flow, and vascular mean transit time. Stroke. 5:630–639.

Hoge RD, Atkinson J, Gill B, Crelier GR, Marrett S, Pike GB. 1999. Linear coupling between cerebral blood flow and oxygen consumption in activated human cortex. Proc Natl Acad Sci USA. 96: 9403–9408.

Horvath I, Sandor NT, Ruttner Z, McLaughlin AC. 1994. Role of nitric oxide in regulating cerebrocortical oxygen consumption and blood flow during hypercapnia. J Cereb Blood Flow Metab. 14: 503–509.

Hyder F, Kida I, Behar KL, Kennan RP, Maciejewski PK, Rothman DL. 2001. Quantitative functional imaging of the brain: towards mapping neuronal activity by BOLD fMRI. NMR Biomed. 14:413–431.

Ito H, Kanno I, Ibaraki M, Hatazawa J, Miura S. 2003. Changes in human cerebral blood flow and cerebral blood volume during hypercapnia and hypocapnia measured by positron emission tomography. J Cereb Blood Flow Metab. 23:665–670.

Ito H, Takahashi K, Hatazawa J, Kim SG, Kanno I. 2001. Changes in human regional cerebral blood flow and cerebral blood volume during visual stimulation measured by positron emission tomography. J Cereb Blood Flow Metab. 21:608–612.

Jacobsen LK, Gore JC, Skudlarski P, Lacadie CM, Jatlow P, Krystal JH. 2002. Impact of intravenous nicotine on BOLD signal response to photic stimulation. Magn Reson Imaging. 20:141–145.

Jones M, Berwick J, Hewson-Stoate N, Gias C, Mayhew J. 2005. The effect of hypercapnia on the neural and hemodynamic responses to somatosensory stimulation. Neuroimage. 27:609.

Jones M, Berwick J, Mayhew J. 2002. Changes in blood flow, oxygenation, and volume following extended stimulation of rodent barrel cortex. Neuroimage. 15:474–487.
Kastrup A, Kruger G, Glover GH, Neumann-Haefelin T, Moseley ME. 1999. Regional variability of cerebral blood oxygenation response to hypercapnia. Neuroimage. 10:675–681.
Kastrup A, Kruger G, Neumann-Haefelin T, Glover GH, Moseley ME. 2002. Changes of cerebral blood flow, oxygenation, and oxidative metabolism during graded motor activation. Neuroimage. 15:74–82.
Kayser C, Petkov CI, Augath M, Logothetis NK. 2005. Integration of touch and sound in auditory cortex. Neuron. 48:373–384.
Kety SS, Schmidt CF. 1945. The determination of cerebral blood flow in man by the use of nitrous oxide in low concentrations. Am J Physiol. 143:53–66.
Kety SS, Schmidt CF. 1947. The effects of altered arterial tensions of carbon dioxide and oxygen on cerebral blood flow and cerebral oxygen consumption of normal young men. J Clin Invest. 27: 484–492.
Kida I, Kennan RP, Rothman DL, Behar KL, Hyder F. 2000. High-resolution CMR(O2) mapping in rat cortex: a multiparametric approach to calibration of BOLD image contrast at 7 Tesla. J Cereb Blood Flow Metab. 20:847–860.
Kim SG, Rostrup E, Larsson HB, Ogawa S, Paulson OB. 1999. Determination of relative CMRO2 from CBF and BOLD changes: significant increase of oxygen consumption rate during visual stimulation. Magn Reson Med. 41:1152–1161.
Kim SG, Ugurbil K. 1997. Comparison of blood oxygenation and cerebral blood flow effects in fMRI: estimation of relative oxygen consumption change. Magn Reson Med. 38:59–65.
Kliefoth AB, Grubb RL, Jr, Raichle ME. 1979. Depression of cerebral oxygen utilization by hypercapnia in the rhesus monkey. J Neurochem. 32:661–663.
Klimscha W, Ullrich R, Nasel C, Dietrich W, Illievich UM, Wildling E, Tschernko E, Weidekamm C, Adler L, Heikenwalder G, et al. 2003. High-dose remifentanil does not impair cerebrovascular carbon dioxide reactivity in healthy male volunteers. Anesthesiology. 99:834–840.
Krnjevic K, Randic M, Siesjoe BK. 1965. Cortical CO2 tension and neuronal excitability. J Physiol. 176:105–122.
Lee SP, Duong TQ, Yang G, Iadecola C, Kim SG. 2001. Relative changes of cerebral arterial and venous blood volumes during increased cerebral blood flow: implications for BOLD fMRI. Magn Reson Med. 45:791–800.
Leontiev O, Buxton RB. 2007. Reproducibility of BOLD, perfusion, and CMRO2 measurements with calibrated-BOLD fMRI. Neuroimage. 35:175–184.
Levin JM, Ross MH, Mendelson JH, Kaufman MJ, Lange N, Maas LC, Mello NK, Cohen BM, Renshaw PF. 1998. Reduction in BOLD fMRI response to primary visual stimulation following alcohol ingestion. Psychiatry Res. 82:135–146.
Liu ZM, Schmidt KF, Sicard KM, Duong TQ. 2004. Imaging oxygen consumption in forepaw somatosensory stimulation in rats under isoflurane anesthesia. Magn Reson Med. 52:277–285.
Logothetis NK, Guggenberger H, Peled S, Pauls J. 1999. Functional imaging of the monkey brain. Nat Neurosci. 2:555–562.
Logothetis NK, Pauls J, Augath M, Trinath T, Oeltermann A. 2001. Neurophysiological investigation of the basis of the fMRI signal. Nature. 412:150–157.
Mandeville JB, Marota JJ. 1999. Vascular filters of functional MRI: spatial localization using BOLD and CBV contrast. Magn Reson Med. 42:591–598.
Mandeville JB, Marota JJ, Kosofsky BE, Keltner JR, Weissleder R, Rosen BR, Weisskoff RM. 1998. Dynamic functional imaging of relative cerebral blood volume during rat forepaw stimulation. Magn Reson Med. 39:615–624.
Metzger H, Heuber S. 1977. Local oxygen tension and spike activity of the cerebral grey matter of the rat and its response to short intervals of O2 deficiency or CO2 excess. Pflugers Arch. 370:201–209.
Nilsson B, Siesjoe BK. 1976. A method for determining blood flow and oxygen consumption in the rat brain. Acta Physiol Scand. 96:72–82.
Novack P, Shenkin HA, Bortin L, Goluboff B, Soffe AM. 1953. The effects of carbon dioxide inhalation upon the cerebral blood flow and cerebral oxygen consumption in vascular disease. J Clin Invest. 32:696–702.
Oeltermann A, Augath MA, Logothetis NK. 2007. Simultaneous recording of neuronal signals and functional NMR imaging. Magn Reson Imaging. 25:760–774.
Ogawa S, Tank DW, Menon R, Ellermann JM, Kim SG, Merkle H, Ugurbil K. 1992. Intrinsic signal changes accompanying sensory stimulation: functional brain mapping with magnetic resonance imaging. Proc Natl Acad Sci USA. 89:5951–5955.
Pattinson KT, Rogers R, Mayhew SD, Tracey I, Wise RG. 2006. Pharmacological FMRI: measuring opioid effects on the BOLD response to hypercapnia. J Cereb Blood Flow Metab. 27:414–423.
Reivich M. 1964. Arterial PCO2 and cerebral hemodynamics. Am J Physiol. 206:25–35.
Roy CS, Sherrington MB. 1890. On the regulation of the blood-supply of the brain. J Physiol. 11:85–108.
Schwarzbauer C, Heinke W. 1999. Investigating the dependence of BOLD contrast on oxidative metabolism. Magn Reson Med. 41:537–543.
Sicard KM, Duong TQ. 2005. Effects of hypoxia, hyperoxia, and hypercapnia on baseline and stimulus-evoked BOLD, CBF, and CMRO2 in spontaneously breathing animals. Neuroimage. 25:850–858.
Sicard K, Shen Q, Brevard ME, Sullivan R, Ferris CF, King JA, Duong TQ. 2003. Regional cerebral blood flow and BOLD responses in conscious and anesthetized rats under basal and hypercapnic conditions: implications for functional MRI studies. J Cereb Blood Flow Metab. 23:472–481.
Siesjoe BK. 1978. Brain energy metabolism. New York: Wiley.
Siesjoe BK. 1980. Cerebral metabolic rate in hypercarbia—a controversy. Anesthesiology. 52:461–465.
Stefanovic B, Warnking JM, Rylander KM, Pike GB. 2006. The effect of global cerebral vasodilation on focal activation hemodynamics. Neuroimage. 30:726–734.
Tombaugh GC, Sapolsky RM. 1990. Mild acidosis protects hippocampal neurons from injury induced by oxygen and glucose deprivation. Brain Res. 506:343–345.
Uludag K, Dubowitz DJ, Yoder EJ, Restom K, Liu TT, Buxton RB. 2004. Coupling of cerebral blood flow and oxygen consumption during physiological activation and deactivation measured with fMRI. Neuroimage. 23:148–155.
Wang Q, Pelligrino DA, Koenig HM, Albrecht RF. 1994. The role of endothelium and nitric oxide in rat pial arteriolar dilatory responses to CO2 in vivo. J Cereb Blood Flow Metab. 14:944–951.
You JP, Wang Q, Zhang W, Jansen-Olesen I, Paulson OB, Lassen NA, Edvinsson L. 1994. Hypercapnic vasodilatation in isolated rat basilar arteries is exerted via low pH and does not involve nitric oxide synthase stimulation or cyclic GMP production. Acta Physiol Scand. 152:391–397.
Zappe AC, Uludag K, Logothetis NK. Forthcoming. 2008. Direct measurement of oxygen extraction with fMRI using 6% CO2 inhalation. Magn Reson Imaging.
Zappe AC, Uludaq K, Rainer G, Logothetis NK. 2005. Influence of moderate hypercapnia on neural activity in monkey by simultaneous intracortical recordings and fMRI at 4.7T. 35th Society for Neuroscience Meeting. 10.11.
Zhu XH, Zhang Y, Tian RX, Lei H, Zhang N, Zhang X, Merkle H, Ugurbil K, Chen W. 2002. Development of (17)O NMR approach for fast imaging of cerebral metabolic rate of oxygen in rat brain at high field. Proc Natl Acad Sci USA. 99:13194–13199.